Finite element /boundary element simulation of future hard disk recording

T. SCHREFL, G. HRKAC, A. GONCHAROV, J. DEAN, S. BANCE, M. A. BASHIR
Department of Engineering Materials
University of Sheffield
Mappin Street, Sir Robert Hadfield Building, Sheffield, S1 3JD
UNITED KINGDOM

D. SUESS
Institute of Solid State Physics
Vienna University of Technology
Wiedner Haupstr. 8-10, 1040 Vienna
AUSTRIA

Abstract: - Future hard disk storage systems will store information at a density of 10 Tbit/in^2. The development and design of high density storage technologies requires the detailed simulation of the magnetization processes. We combine a hybrid finite element/boundary element method with matrix compression techniques and fast Poisson solvers, in order to simulation the writing process on a magnetic hard disks.

Key-Words: - micromagnetics, hard disk storage, finite element method, fast boundary element method, object oriented design

1 Introduction

The design and optimization of ultra high density storage technologies requires a precise understanding of the dynamics of magnetization reversal in hard disk systems. These include the magnetic storage layer itself, the magnetic write head with current carrying coils, and any additional magnetic layers, like the soft magnetic underlayer (SUL) that enhances the writeability. In addition to the write process that needs a careful design of all interaction parts, the thermal stability becomes a main issues in future magnetic recording. A route to optimize and improve hard disk systems is micromagnetic simulation. Micromagnetism [1] is a continuum theory that describes the dynamics of the magnetization. By solving an equation of motion for the magnetization vector the magnetic state of a material can be predicted as function of space and time. The main challenge for the numerical solution is the huge change in characteristic length scales of the systems involved ranging from sub-nanometers to several micrometers. Current roadmaps in magnetic data storage aim for a storage density of 10 Tbit/in^2. This will require magnetic islands of 6 nm x 6 nm with a non-magnetic spacer between the islands of 2 nm. Each island itself will be composed of multiple magnetic layers with a thickness of 2 nm or less. The writer dimensions including the coil exceed easily 10 micrometers. The design of recording devices requires the span a length scale of more than four orders of magnitude as the interaction between all parts (storage layers, soft underlayer, write head, shields, and coil) has to be taken into account. We developed a finite element / boundary element method in order to span length scales over four orders of magnitude as required for this type of simulations.

This paper is organized as follows. We first give an introduction into the current state of the art of magnetic hard disk storage in section 2. In section 3 we present the governing equations that have to be solved. Section 4 deals with the set of numerical methods that are combined to effectively simulate the write process and the thermal stability of future hard disk systems. We apply a finite element method for space discretization, a fast boundary method to treat the magnetic interaction between moving parts, and a fast Poisson solver to evaluate the magnetostatic fields. Section 5 presents numerical results for recording on bit patterned media.

2 Recording technologies

Current hard disk technology uses perpendicular magnetic recording media. Data is stored using granular magnetic thin films with the magnetically easy axis perpendicular to the film plane. With the last two years, the transition from longitudinal magnetic recording to perpendicular magnetic recording took place. All major

recording companies are now shipping products based on perpendicular magnetic recording.

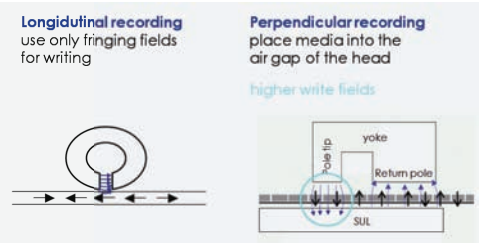

Fig 1. Transition from longitudinal to perpendicular recording. In perpendicular recording information is stored using magnetic moments pointing perpendicular to the thin film. One major advantage of perpendicular recording is the possibility to use higher write fields which results in a gain of in thermal stability and consequently area density.

A major limit in conventional magnetic recording technology is given by the superparamagnetic effect. When the magnetic storage unit becomes too small the magnetization will lose its preferred direction due to thermal fluctuations. In order to achieve a high signal to noise ratio on bit of a magnetic recording medium is made of several storage units (grains). By making the bit size smaller the grain size has to decrease as well, in order to keep a sufficient number of grains per bit. In order to avoid thermal decay of the information, the magnetocrystalline anisotropy of the material has to be increased. A high magneto-crystalline anisotropy keeps the magnetization stable against thermal fluctuations but also increases the magnetic field required to reverse the magnetization. This effect provides the ultimate limit for storage density in conventional perpendicular recording. At some stage, the field produced by the write head is just too small to switch the grains and write information onto the disk. By placing the media effectively into the air gap of the writer (write pole, yoke, soft under layer, and return pole) a higher write field can be achieved in perpendicular magnetic recording as compared to longitudinal recording which can make only use of the fringing fields of the writer (see Fig 1). The higher write field is one of the main advantages of perpendicular recording. It is now possible to shrink the grains while keeping a high thermal stability by increasing the magnetocrystalline anisotropy. The interplay between signal to noise, thermal stability, and writeability is usually referred to as recording trilemma [2].

Conventional perpendicular magnetic recording is believed to reach recording densities in the range of 500 Gbit/in^2 to 600 Gbit/in^2 [3]. At 500 Gbit/in^2 one bit covers an area of about 17 nm x 75 nm. One bit is made out of an ensemble of grains with a diameter in the range of 6 nm to 8 nm. At 500 Gbit/in^2 one bit is made of about 30 grains with their magnetization point in the same direction, either up or down. Recent Lab demonstrations come close to the limit of conventional perpendicular recording. In October 2007, Western Digital announced an area density of 520 Gbit/in^2 [4].

One way to overcome the recording is so-called bit patterned media. The key idea of bit patterned recording is to increase the volume of a magnetic storage unit and thus make it thermally more stable. This increases the product of the magnetic anisotropy energy (anisotropy energy density multiplied by volume) of the magnetic entity and thus enhances the thermal stability. Increasing the grain size in granular thin film media to increase the volume of magnetic entity in granular thin film recording media would increase the noise and broaden the transition width between bits. If the bit boundary is broad the bits cannot put closely together leading to transition jitter. In bit patterned media the bit boundary is defined by patterning. The magnetic entities are physically separated and the transition jitter is reduced.

3 Micromagnetic equations

A magnetic material can be characterized by the spatial distribution of its magnetic polarization vector. The equilibrium configuration of the magnetic polarization can be directly computed by minimizing the total magnetic Gibb's free energy. The total Gibb's free energy is the sum of the exchange energy, the magneto-crystalline anisotropy energy, the magnetostatic energy, and the Zeeman energy:

$$E_t = \int \left[A \sum_{i=1}^{3} (\nabla \beta_i)^2 + f_k(\boldsymbol{J}) - \frac{1}{2}\boldsymbol{J}\cdot\boldsymbol{H}_{\mathrm{d}} - \boldsymbol{J}\cdot\boldsymbol{H}_{\mathrm{ext}} \right] dV, \qquad (1)$$

where $\boldsymbol{J} = (\boldsymbol{\beta}_1,\boldsymbol{\beta}_2,\boldsymbol{\beta}_3)J_s$ denotes the magnetic polarization. A is the exchange constant and f_k is the energy density associated with the uniaxial magnetocrystalline anisotropy of grains in the magnetic storage layer. $\boldsymbol{H}_{\mathrm{d}}$ and $\boldsymbol{H}_{\mathrm{ext}}$ denote the demagnetizing and the external field, respectively. The minimization of (1) with respect to $\boldsymbol{J}$, subject to the constraint $|\boldsymbol{J}| = J_s$, provides an equilibrium state of the ferromagnetic structure. However, in magnetic recording we are also interested in the time evolution of the magnetic polarization. Here the external field is a function of time $\boldsymbol{H}_{\mathrm{ext}} = \boldsymbol{H}_{\mathrm{ext}}(t)$ and is generated by a current pulse through the coil of the magnetic write head.

The Gilbert equation of motion

$$\frac{\partial \boldsymbol{J}}{\partial t} = -|\gamma|\boldsymbol{J}\times(\boldsymbol{H}_{\mathrm{eff}} + \boldsymbol{H}_{th}) + \frac{\alpha}{J_s}\boldsymbol{J}\times\frac{\partial \boldsymbol{J}}{\partial t}, \qquad (2)$$

gives the dynamic response of the magnetization due to a change of the driving field $\boldsymbol{H}_{\mathrm{ext}}$. The effective field $\boldsymbol{H}_{\mathrm{eff}}$ is the negative variational derivative of the magnetic

Gibb's free energy density. $\boldsymbol{H}_{\text{th}}$ is a random, thermal field that mimics the effect of thermal fluctuations at non-zero temperature assuming white noise. The thermal field has zero mean and is uncorrelated in time and space.

The external field is the magnetic field created by a given current distribution. Examples are the current through the driving coil of the write head or the current through the sensing element of a read head. It can be calculated by Bio-Savart's law

$$\boldsymbol{H}_{\text{exl}}(\mathbf{r}) = \frac{1}{4\pi}\int_V \mathbf{j}\times\frac{\mathbf{r}-\mathbf{r}'}{|\mathbf{r}-\mathbf{r}'|^3}dV', \tag{3}$$

where the integral is over the conductor with a current density **j**. The numerical evaluation of (3) for the calculation of the field created from current coils uses matrix compression techniques that will be discussed in later in section 4.

The demagnetizing field $\boldsymbol{H}_{\text{d}}$, which is also called magnetostatic interaction field, follows from a magnetic scalar potential *u*

$$\Delta u = \frac{\nabla \boldsymbol{J}}{\mu_0} \text{ and } \boldsymbol{H}_{\text{d}} = -\nabla u \tag{4}$$

The right hand side of equation (4) is zero for any point outside the magnetic materials. Equation (4) is an open boundary problem [5]. There is no boundary conditions that gives the potential at the surface of the magnet. For the unique solution of (4) one need to apply the condition that *u* approaches zero at infinity. We use a hybrid finite element / boundary element method to solve (4) whereby significant speed up and memory reduction is obtained using matrix compression.

4 Numerical methods

Fig. 2 illustrates the multiscale nature of magnetic recording simulations. The length scales span several orders of magnitude. In addition we have to treat moving parts as the head is flying over the data layer during magnetic recording.

We use an object oriented approach to represent the different real world objects and their interactions. The basic objects of the simulation software are shown in Fig. 3. The interaction objects take care of the mutual interactions between the models. Magnets and conductors are generalized as model. Each model has its locally changing material properties (grains), a finite element mesh, magnetic moments, and effective fields. For fast computation of the interaction fields the mesh points are divided into clusters. The field box is used for field evaluation using a fast Poisson solver.

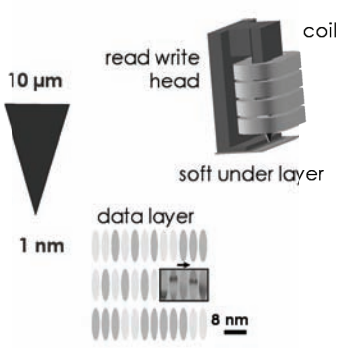

Fig 2. Multiscale simulation of high density magnetic recording systems. The characteristic length scale ranges from more than 10 nm in coils to 1 nm size features in the data layer.

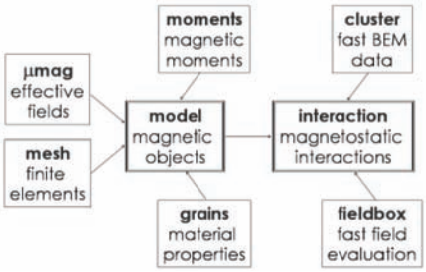

Fig. 3. Objects in magnetic recording simulations.

4.1 Models – space discretization

Each part of the recording system (coil, yoke and pole tip of the write head, data layer, and soft underlayer) is treated as a model. In order to represent the magnetization distribution within a magnetic model, we mesh the model using a tetrahedral mesh. Within a tetrahedron the Cartesian components of $\boldsymbol{J}$ are interpolated with linear basis functions. Each node point holds a magnetic moment vector $\boldsymbol{m}_i = \boldsymbol{J}V_i/\mu_0$ and an effective field vector $\boldsymbol{H}_{\text{eff},i}$. Here μ_0 is the permeability of vacuum. The effective field $\boldsymbol{H}_{\text{eff}}$ at the nodal points of the finite element mesh is calculated within the framework of the box method. At the nodal point *i* of the finite element mesh is approximated by [6]

$$\boldsymbol{H}_{\text{eff},i} = -\frac{1}{V_i}\frac{\partial E_t}{\partial \boldsymbol{J}} \tag{5}$$

where V_i is the volume of a "box" surrounding the nodal point *i*. The box volumes are mutually exclusive so that the following equation holds

$$\sum_j V_j = V \text{ and } V_i \cap V_j = 0 \text{ for } i \neq j. \tag{6}$$

Similarly the coil is meshed into tetrahedral elements. Here the current density **j** is defined at the nodes of the mesh.

Some of the magnetic layers in magnetic recording system such as the soft underlayer are artificial antiferromagnets. Two ferromagnetic layers are separated by a very thin (0.8 nm) Ru layer that introduces an antiferromagnetic coupling between the two ferromagnets. This trick proved to be efficient in order to avoid spurious magnetic fields caused by moving magnetic domain walls. We use special finite elements that were originally developed to model thin air gaps in magnetostatic field calculations [6], in order to treat such thin layers. These shell elements are triangular prism element with no volume. The integration along the direction perpendicular to the thin layer is performed analytically before the system matrices are built.

4.2 Interactions – magnetic field computation

In order to simulate the recording process we have to treat the motion of the writer over the magnetic storage layer. A common approach to include moving parts into electromagnetic finite element simulations is the use of sliding grids and Mortar elements [7]. An alternative approach is the use of the use hybrid finite element / boundary element (FEM/BEM) techniques [8]. For magnetic recording simulations FEM/BEM methods have the advantage that no mesh is needed between the different magnetic parts, and the magnetization dynamics can be calculated in the rest frame of each part.

Further, the FEM/BEM method effectively treats the open boundary problem, since it takes the boundary condition $u = 0$ at infinity into account. For the solution of equation (4) with the hybrid FEM/BEM method one Poisson equation with Neumann boundary conditions and one Laplace equation with Dirichlet boundary conditions have to be solved. To obtain the boundary conditions a matrix vector product has to be performed. We split the total magnetic potential u into two parts, $u = u_1 + u_2$. The potential u_1 solves the Poisson equation (4) inside the magnetic particles with Neumann boundary conditions at the surface of the magnets and it is zero outside the magnets. The potential u_2 solves the Laplace equation everywhere in space and shows a jump at the surfaces of the magnets. The potential u_2 is the potential from a magnetic dipole sheet at the surfaces of the magnet and can be computed by a surface integral over the boundary. After discretization the integral operator may be expressed as a matrix vector product

$$\boldsymbol{u}_2 = B\boldsymbol{u}_1 \tag{7}$$

Here $\boldsymbol{u}_1$ and $\boldsymbol{u}_2$ are vectors that collect the potential values at the surface nodes of the finite element grid. The storage requirement for the matrix B is the bottleneck of the method since is a fully populated matrix. The storage requirements and computational costs are of $O(M^2)$, where M is the number of boundary nodes. Especially for magnetic thin films the method loses efficiency since most of the nodes are located at the boundary.

4.2.1 Clusters

The idea of clustering the surface nodes of the surface mesh allows the storage of the boundary matrix in compressed form. The compressed matrix is sparse in a sense that only few data are needed for its representation. The matrix–vector multiplication is of almost linear complexity [9]. Originally, the discretization of the boundary integral leads to a large dense matrix that has no explicit structure. However, by suitable renumbering and permuting the boundary nodes, the dense matrix can be written in a block structure so that each block describes the interaction between two clusters of boundary nodes. If the two clusters are far apart the corresponding block matrix can be approximated by low rank matrices. The corresponding two clusters are called admissible. If the $n \times m$ matrix D is a block matrix that describes the interaction of two admissible clusters it can be approximated

$$D_{nm} = \sum_{i=1}^{k} E_{ni} F_{im} \tag{8}$$

by the product of two smaller matrices with the dimensions $n \times k$ and $k \times m$. For admissible clusters k will be much smaller than n and much smaller than m. Therefore both, the storage for the block matrix and CPU time evaluating the product of the block matrix vector with a vector is only $O(k(n+m))$ instead of $O(nm)$.

The renumbering of the nodes is done by geometric criteria. Consecutive boundary node numbers will be assigned to nodes located close to each other. These nodes are combined in a cluster. Each cluster pair corresponds to a block in the renumbered boundary matrix. Two admissible clusters appear as a large off-diagonal block matrix can be approximated by a product of two smaller matrices. The off-diagonal blocks represent the far field interactions between nodes. Fig. 4 gives an example for the panel clustering and the block structure for a set of 10 nodes. The cluster with the nodes (8,9,10) and the cluster with the node (1,2,3,4,5) form a pair of admissible clusters. The corresponding block matrix appears in the lower left corner of the boundary matrix.

There is no need to compute the full matrix in order to evaluate the matrix vector product (7). First, the boundary nodes are renumbered and arranged into a cluster tree. Then, the low rank approximation of the

off-diagonal block matrices can be computed using adaptive cross approximation [10]. This iterative algorithm computes factorization (8) of the block matrix into two smaller matrices with a complexity of $O(k^2(n+m))$.

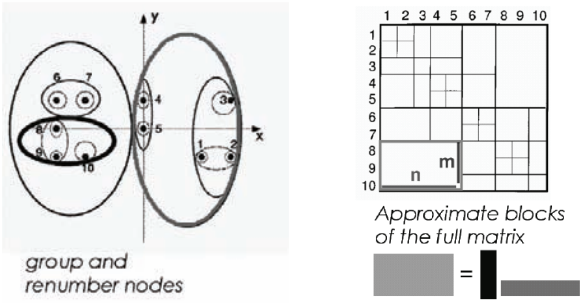

Fig. 4. Fast boundary element method used for the calculation of magnetostatic interactions. Left hand side: The nodes are renumbered and grouped together so that nodes with consecutive numbers are located next to each other and form a cluster. Right hand side: Corresponding block structure of the interaction matrix. The large off-diagonal blocks can be approximated by low rank matrices. After [10].

4.2.2 Fieldboxes and moving parts

Equation (7) also treats the interactions between distinct magnetic parts. This leads to the complication that the interaction matrix has to be re-evaluated at each time step. Despite the gain in CPU time owing to matrix compress the repeated computation of the interaction matrix is too costly for recording simulations. In order to avoid this problem we use the properties of the magnetic scalar potential. For example, the scalar potential produced by the head magnetization follows from a surface integral over the surface of the head. Instead of evaluating the potential directly on the nodes of the storage layer, we evaluate the potential at the surface of a field box that encloses the storage layer. Then a fast Poisson solver is used to compute the potential from the head within the field box at high spatial resolution. Numerical derivation gives the magnetostatic field on the field box grid. Finally, the magnetostatic interation field in the storage layer is computed by interpolation from the regular grid of the box onto the finite element mesh of the storage layer.

Again, we use matrix compression techniques to reduce the size of the interaction matrix, which relates the surface nodes of the head with the surface nodes of the field box. The idea of clustering the surface nodes of the surface mesh allows the storage of the boundary matrix in compressed form.

4.3 Time integration

The space discretization described above leads to a system of ordinary differential equations (ODEs). The ODEs describe the dynamics of the magnetic moments at the nodes of the finite element mesh. Owing to ferromagnetic exchange that strongly couples neighboring magnetic moments and favors their parallel orientation the ODEs are stiff. Therefore we use a backward differentiation scheme [11]. It is essential to apply a proper preconditioner. We provide an approximate Jacobian matrix that contains all the short-range interactions (ferromagnetic exchange interactions, magnetocrystalline anisotropy, external field) but neglects the long-range magnetostatic interactions. This method speeds up the time integration by orders of magnitude [12].

5 Results

One serious problem in bit patterned magnetic recording is write synchronization. The write field has to hit the magnetic island at exactly the right time. If the write field switches to early or to late the target island will be missed and no bit is written. Schabes [13] introduced the concept of addressability for bit patterned recording. Switching of a given island is possible within a certain write margin. Magnetostatic interactions amongst the islands create additional fields acting on the target island during writing. As a consequence the write margin will depend on the magnetic state.

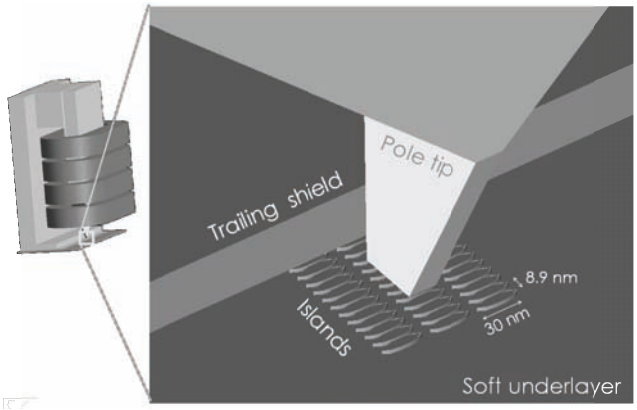

Fig. 5. Write head and magnetic elements for bit patterned recording. The image shows a blow-up of the region below the pole tip of the head.

We compute the write margins for a given random magnetization configuration in patterned media with a storage density of 2 Tbit/in^2. The media design follows that proposed by Richter and co-workers [14]. The islands were of ellipsoidal shape with a length of 30 nm and a width of 7.5 nm. The center to center spacing was 8.98 nm. The switching field of the island is around 1 T

with a minimum at a field angle of about 40 degree. The island thickness was 3 nm, the air bearing surface (ABS) to media spacing was 3 nm and the ABS to soft underlayer (SUL) spacing was 8 nm. Recording simulations were performed using a standard single pole head with trailing shield. We calculated the maximum write margins including magnetostatic effects (interactions between the dots and head-media-head interactions). The multiscale nature of the simulation project becomes clear by looking at the writer and the patterned elements simultaneously (Fig. 5).

To compute the write margins we were running the simulations several times with different initial positions of the head. To avoid any effects from the head dynamics we first computed the remanent state of the head, then cycled the head several times and finally performed the recording simulations. With a data rate of 2 bits per nanosecond the head velocity used in the simulations was 17.96 m/s. From the results we conclude that the non-uniform magnetization reversal of the dots and the magnetostatic interactions between the dots narrow the write margin. Most of the dots are multi-domain for an extended time period before they reach their final magnetic state (up or down). Fig. 6 shows the successful writing of bits in the center track in an array of 3 x 12 magnetic islands. The write margin was found to be 1.75 ± 0.25 nm. This corresponds to 19 percent of the center to center spacing of the dots. Moving the head out of phase by more than 1.75 nm leads to bit errors. Bit errors especially are found for bits where the stray field from the neighboring track is high.

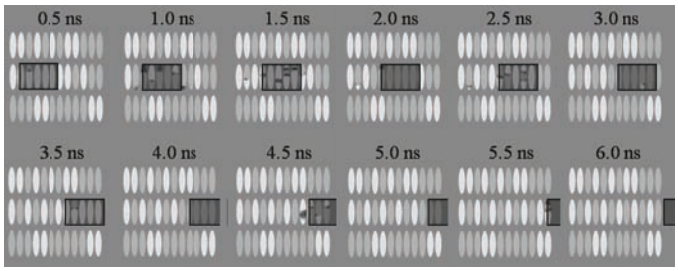

Fig. 6. Successful writing on bit patterned magnetic recording media. Magnetization reversal of the island occurs by the nucleation of a reversed domain and successive domain wall motion. The shaded area denotes the position of the pole tip of head.

6 Conclusion

We presented numerical methods for magnetic recording simulations. The mutual interaction between moving parts is efficiently treated using a hybrid finite / element boundary method. The adaptive cross approximation scheme is used to compress the interaction matrices.

Work supported by the INSIC EHDR programme.

References:

[1] A. Aharoni, *Introduction to the Theory of Ferromagnetism*, Oxford University Press, 1996.

[2] H. J. Richter, The transition from longitudinal to perpendicular recording, *J. Phys. D: Appl. Phys.*, VOL. 40, 2007, pp. R149-R177.

[3] S. N. Piramanayagam, Perpendicular recording media for hard disk drives, *Journal of Applied Physics*, VOL. 102, 2007, 011301.

[4] 520 Gb/in^2 Areal Density in Demonstration, *Company Achieves*, http://www.wdc.com/, November 29, 2007.

[5] Q. Chen, A. Konrad, A review of finite element open boundary techniques for static and quasi-static electromagnetic field problems, *IEEE Trans. Magn.*, VOL. 33, 1997, pp. 663-676.

[5] C. W. Gardiner, *Handbook of stochastic methods*, Springer, 1985.

[6] C. Guérin, G. Tanneau, G. Meunier, X. Brunotte, and A. Jean-Baptiste, Three dimensional magnetostatic finite elements for gaps and iron shells using magnetic scalar potentials, *IEEE Trans. Magn.*, VOL. 30, 1994, pp. 2885-2888.

[7] A. Buffa, Y. Maday, F. Rapetti, A sliding mesh-mortar method for a two dimensional eddy currents model of electric engines, *Meth. Math. En. Anal. Num.*, VOL. 35, NO. 2, 2001, pp. 191-228.

[8] D. R. Fredkin and T. R. Koehler, Hybrid Method for Computing Demagnetizing Fields," *IEEE Trans. Magn.*, VOL. 26, 1990, pp. 415-417.

[9] L. Grasedyck, W. Hackbusch, Construction and arithmetics of H-matrices, *Computing*, VOL. 70, 2003, pp. 295-334.

[10] S. Kurz, O. Rain, and S. Rjasanow, The Adaptive Cross-Approximation Technique for the 3-D Boundary-Element Method, *IEEE Trans. Magn.*, VOL. 38, 2002, pp. 421-424.

[11] G. D. Byrne and A. C. Hindmarsh, PVODE, An ODE Solver for Parallel Computers, *Int. J. High Perf. Comput. Appl.*, VOL. 13, 1999, pp. 354-365.

[12] D. Suess, V. Tsiantos, T. Schrefl, J. Fidler, W. Scholz, H. Forster, R. Dittrich, and J. J. Miles, Time resolved micromagnetics using a preconditioned finite element method, *J. Magn. Magn. Mater.*, VOL. 248, 2002, pp. 298-311.

[13] M. E. Schabes, Micromagnetic Simulations for Terabit/in2 Head/Media Systems, *Journal of Magnetism & Magnetic Materials*, PMRC 2007, Tokyo, 2017pB-2001 (2008).

[14] H. J. Richter, A. Y. Dobin, R. T. Lynch, D. Weller, R. M. Brockie, O. Heinonen, K. Z. Gao, J. Xue, R. J. M. v d Veerdonk, P. Asselin, M. F. Erden, Recording potential of bit-patterned media, *Appl. Phys. Lett.*, VOL. 88, 2006, 222512.